EUROPEAN JOURNAL OF PURE AND APPLIED MATHEMATICS
2025, Vol. 18, Issue 3, Article Number 6341
ISSN 1307-5543 – ejpam.com
Published by New York Business Global

An Exploration of the Topological Structure and Bifurcation of Liouville Tori in Models of Galactic Motion

T. S. Amer[1,*], F. M. El-Sabaa[2], M. Fakharany[1,3], H. M. Gad[2]

[1] *Department of Mathematics, Faculty of Science, Tanta University, Tanta 31527, Egypt*
[2] *Department of Mathematics, Faculty of Education, Ain Shams University, Cairo, Egypt*
[3] *Mathematics and Statistics Department, College of Science, Taibah University, Yanbu, Saudi Arabia*

Abstract. This paper examines two integrable cases: a generalized Hénon-Heiles (HH) system and a quartic potential. For each case, the Liouville tori's bifurcation (LTB) is analyzed. Periodic solutions (PS) are derived using Jacobi elliptic functions, and the corresponding phase portraits are presented with a classification of the singular points. Furthermore, the PS for both cases is constructed based on the Lyapunov theorem. The possible applications of this study are primarily confined to celestial mechanics and astrodynamics. Specifically, the generalization of the HH system and quartic potentials often appears in modeling gravitational interactions between celestial bodies, including the study of the stability and motion of planets, asteroids, and satellites. Additionally, the classification of singular points and phase portraits provides valuable insights for identifying chaotic or regular behaviors in various systems, such as weather models or economic systems. Furthermore, understanding bifurcations and PS contributes to the design of control mechanisms for nonlinear systems, including robotics and automated processes.

2020 Mathematics Subject Classifications: 37J35, 70H06, 37G10, 70F15

Key Words and Phrases: Hamilton-Jacobi Equations, Lyapunov's method, Level sets'topology, Periodic solution, Phase portrait

1. Introduction

In the current paper, we will discuss the two models of galactic motion to get a complete description of these motions in view of studying the bifurcation and the topology of invariant level sets (LS) of the separated functions namely, the third case of the generalized HH and the non separated case of the quartic potential function (PF).

*Corresponding author.
DOI: https://doi.org/10.29020/nybg.ejpam.v18i3.6341

Email addresses: tarek.saleh@science.tanta.edu.eg (T. S. Amer), fawzyfahmy@edu.asu.edu.eg (F. M. El-Sabaa), mohamed.elfakharany@science.tanta.edu.eg, fakharany@aucegypt.edu (M. Fakharany), hadeermahmoud@edu.asu.edu.eg (H. M. Gad)

The axisymmetric PF of the movement of a star around the galactic center in the system of HH takes the following form

$$V = \frac{1}{2}r^2 - \frac{1}{3}r^3 \cos 3\theta.$$

This function is specified by 3-D cylindrical coordinates, where one of them is cyclic, and the problem is reduced to the plane motion. The Hamiltonian function associated with the potential V is

$$H = \frac{1}{2}\left(P_X^2 + P_Y^2 + X^2 + Y^2\right) + XY^2 - \frac{1}{3}X^3.$$

This system can be integrated numerically for a fixed value of total energy, where there exists an invariant torus around the PS of the system, while the motion exhibits large stochasticity as the constant of energy increases. Hénon and Heiles [1] claim that there is no change with the addition of potential higher-order terms, while Contopoulos and Polymilis [2] demonstrated that the HH potential is considered as Toda's lattice third-order term that can be integrable in a 2-D system [3]. The generalized HH can be taken the form

$$H = \frac{1}{2}\left(P_X^2 + P_Y^2 + c_1X^2 + c_2Y^2\right) + aXY^2 - \frac{b}{3}X^3. \tag{1}$$

A large number of articles have been studied with the generalized HH. In [4], the second-order averaging method with a small parameter is utilized to investigate the existence of PS families under specific parameter conditions, characterizing the stability of periodic orbits. Melnikov's method, as applied in [5], confirms the non-integrability of neighboring HH systems and determines the width of the principal chaotic layer responsible for this behavior. In [6], second-order averaging theory is applied to study periodic orbits in generalized HH systems. Furthermore, in quantum mechanics, the HH model serves as a representation of atomic oscillators in triatomic molecules. In [7], the nonlinear HH system is analyzed to study the wave packet behavior of bound states and the connection between quantum and classical dynamics. Meanwhile, [8] investigates the non-uniform motion of charged particles in a crystal under the HH potential. The other model of study in this article is the quartic PF, which can be taken in the form

$$V = \alpha x^4 + \delta x^2y^2 + \beta y^4. \tag{2}$$

By adding two coupled quadratic harmonic oscillators $\omega x^2 + \sigma y^2$ to the function V, then we have a model which was studied in several fields in physics: in quantum mechanics and quantum field theory, see [9], in chemical physics [10] and in scalar field theory as presented in [11]. In galactic motion, the model has been studied by many authors. Pucacco et al.[12] studied the galactic potential (GP) $V(x^2, y^2)$ which is the modeling of elliptical galaxies. The Armbruster- Guckenheimer-Kim (AGK) potential [13] is another model that consists of a 2-D harmonic potential with quartic terms. Friedmann-Roberston-Walker (FRW) potential was introduced in [14], a model of GP, which modulates containing a positive or

negative gravitational coupled scalar field in the loop quantum cosmology scenario.

By using Painlevé property [15, 16], the generalized HH system and quartic potential can be integrated for the special values of constants as follows:

In generalized HH:
(i) $b/a = -1$, $c_1 = c_2$, (ii) $b/a = -6$, $\quad c_1,\ c_2$ arbitrary, (iii) $b/a = -16$, $c_1 = 16c_2$.
For quartic potential:
(i) $\alpha = \beta,\ \delta = 6\beta,$ (ii) $\alpha = \beta,\ \delta = 2\beta$, (iii) $\beta = 16\alpha,\ \delta = 12\alpha$, (iv) $\beta = 8\alpha,\ \delta = 6\alpha$,
where there exists an invariant torus around the PS of the system. It is well known that the first two cases of generalized HH and the first three cases of quartic potential have been separated, and the second invariant integrals was given in quadratic in momenta see for instance [15–20]. There are some problems in which the conditions for integrability have been defined, but separation has not been achieved. The last cases of generalized HH and quartic potential are belonging to this group, where the invariant integral for both cases is quartic in momenta

$$I_{GHH} = P_Y^4 + 2Y^2(c_2 + 2aX)P_Y^2 + c_2^2Y^4 - \tfrac{4}{3}a\left(\left(P_XP_Y + \tfrac{a}{6}Y^3\right)Y^3 + (c_2 + aX)XY^4\right),$$
$$I_{quad} = p_x^4 + 4x^2(x^2 + 6y^2)p_x^2 + 4x^4p_x^2 - 16x^3yp_xp_y + 4x^4(x^4 + 4x^2y^2 + 4y^4).$$

If there is a second independent invariant integral, then the 2-DOF system is integrable. The second invariant can be given by different methods: Whittaker [21] considered the invariant integral which is quadratic in momenta, and he studied some special cases to get the integral. Dorizzi et al. [22] applied the Whittaker-Daraboux equation, and by rotation of the coordinates, they introduced a partial differential equation in the form

$$2xV_{xy} + 3V_y + y(V_{yy} - v_{xx}) = 0, \tag{3}$$

with the Hamiltonian function $H = \frac{1}{2}(p_x^2 + p_y^2) + V(x, y)$, and they proved that there exists a second invariant of motion which is quadratic in momenta. The solutions of the equation (3) are given in several classes of the homogenous PF $V_s(x, y)$:

$$V_0 = 1, \quad V_1 = 2x, \quad V_2 = 4x^2 + y^2,$$
$$V_3 = 8x^3 + 4y^2x, \quad V_4 = 16x^4 + 12x^2y^2 + y^4.$$
$$etc..$$

Nakagawa and Yoshida [23] considered a homogeneous PF

$$V_s = \frac{1}{r}\left(\left(\frac{r+x}{2}\right)^{s+1} + (-1)^s\left(\frac{r-x}{2}\right)^{s+1}\right), \quad r^2 = x^2 + y^2,$$

is separable in parabolic coordinates $\tau = \frac{r+x}{2}$, $\quad \sigma = \frac{r-x}{2}$, and the invariant integral I_s is given by

$$I_s = p_y(yp_x - xp_y) + \frac{1}{2}y^2V_{s-1},$$

where the explicit functions

$$V_2 = \frac{1}{4}(4x^2 + y^2), \quad V_3 = \frac{1}{8}(8x^3 + 4xy^2), \quad V_4 = \frac{1}{16}(16x^4 + 12x^2y^2 + y^4).$$

It is clear that both mentioned methods can not give the separability of the last two cases of generalized HH and quartic potential. Verhoeven et al. [24] used the general solution for the Kaup-Kupershmidt (KK) to get a separation of the variables for the third case of generalized HH, while Ravoson et al. [25] used the method described by Vanhaecke [26] to get the separability of the last case of the quartic potential.

The primary objective of this research article is to comprehensively elucidate the problem under investigation through an examination of the bifurcation and the topology of invariant LS of the separated functions employing Fomenko's theory [27]. In [28], the Fomenko classification is applied to the two fixed centers problem, while in [29], the bifurcation behavior of the AGK GP is investigated. Waalkens et al. [30] investigated the topology of energy surface bifurcations during three-dimensional motion. The bifurcation of a common level set was studied in [31] for the first integral of Kovalevskaya problem, while the LTB of the problem of the rigid body (RB) rotation around a fixed point in different cases is obtained in [32]. In [33], the author investigated the RB motion while it is affected by restoring, perturbing, and gyrostatic moments. In [34], it is expected that the gyro's direction is near the axis of dynamic symmetry, its angular velocity is sufficiently large, and its perturbing moments are minimal in relation to its restoring ones. These circumstances allow for the introduction of a tiny parameter. In the first and second approximations, averaged systems of the equations of motion are found. In [35], the authors used Taylor and the average methods to solve the problem while the body contained a cavity filled with fluid and impacted by gyrostatic and constant torques.

The current paper is constructed as outlined below: In section 2, the separation of the third case of generalized HH problem is introduced, and the topology of invariant LS of the separated functions is discussed in subsection 2.1 using Fomenko's classification theorem [27]. Subsection 2.2 investigates the PS for singular LS of bifurcation. In subsection 2.3, the phase portrait of the separation functions is introduced, and the singular points and their types are obtained. In section 3, the separation for the last case of quartic potential (2) is examined, and the topology of real phase space and the sets of bifurcation are investigated in subsection 3.1. The PS is examined in subsection 3.2. The separated function is used in subsection 3.3 to examine the system's phase portrait and discover the various forms of singular points. In section 4, we obtain the PS about the equilibrium points.

This study finds applications in celestial mechanics and astrodynamics, where generalized HH-systems and quartic potentials are used to model gravitational interactions among celestial bodies. These models help analyze the stability and motion of planets, asteroids, and satellites. Moreover, the classification of singular points and phase portraits aids in identifying chaotic or regular behaviors in complex systems like weather models and economic frameworks. The insights into bifurcations and PS further enable the design of control mechanisms for nonlinear systems such as robotics and automation.

2. Separation of the third case of generalized HH

Hamiltonian function for generalized HH has the form

$$H = \frac{1}{2}\left(P_X^2 + P_Y^2 + c_1X^2 + c_2Y^2\right) + aXY^2 - \frac{b}{3}X^3.$$

It is shown in [36] that the three cases of generalized HH can be related to the Sawada-Kotera (SK), KdV5, and equations of KK, respectively. Verhoeven et al. [24] used the KK equations to get the separate functions of the Hamiltonian for the third case of generalized HH, which is based on the following values of parameters

$$a = \frac{1}{4}, \quad c_1 = 16c_2, \quad c = c_1c_2,$$

with the transformation $u = X + 2c_2$, and $v = Y$.
After performing the mathematical operations, they obtained the Hamiltonian

$$H = \frac{1}{2}(p_u^2 + p_v^2) + \frac{1}{4}uv^2 + \frac{4}{3}u^3 - cu. \tag{4}$$

Finally, the following transformation is used to get the separable Hamiltonian function

$$\begin{aligned}
q_1 &= -6\tfrac{p_v^2 - k_{2,0}}{v^2} - u,\\
q_2 &= -6\tfrac{p_v^2 + k_{2,0}}{v^2} - u\\
p_1 &= \tfrac{1}{2v^3}\left(12p_v^3 + 6uv^2p_v - v^3p_u - 12p_vk_{2,0}\right),\\
p_2 &= \tfrac{1}{2v^3}\left(12p_v^3 + 6uv^2p_v - v^3p_u + 12p_vk_{2,0}\right).
\end{aligned}$$

Therefore the Hamiltonian system (4) takes the form

$$H = p_1^2 + p_2^2 + \frac{1}{12}(q_1^3 + q_2^3) - \frac{c}{4}(q_1 + q_2). \tag{5}$$

Using Hamilton Jacobi equations

$$h + \left(\frac{\partial W}{\partial q_1}\right)^2 + \left(\frac{\partial W}{\partial q_2}\right)^2 + \frac{1}{12}(q_1^3 + q_2^3) - \frac{c}{4}(q_1 + q_2) = 0, \tag{6}$$

where W is a complete integral and it has the form

$$W = W_1(q_1) + W_2(q_2). \tag{7}$$

Thus, equation (6) can be introduced as

$$\begin{aligned}
2\left(\tfrac{dW_1}{dq_1}\right)^2 + \tfrac{q_1^3}{6} - \tfrac{c}{2}q_1 + h &= \alpha,\\
2\left(\tfrac{dW_2}{dq_2}\right)^2 + \tfrac{q_2^3}{6} - \tfrac{c}{2}q_2 + h &= -\alpha,
\end{aligned} \tag{8}$$

and W can be obtained in the following form

$$W = \int \sqrt{\phi(z)}dz, \tag{9}$$

where

$$\phi(z) = \pm 2\alpha - 2h - \frac{z^3}{3} + cz, \quad z = z(q_1, q_2). \tag{10}$$

Thus, the differential equation can be written as

$$\frac{dz}{\sqrt{\phi(z)}} = t - t_0. \tag{11}$$

2.1. Topological analysis

The Fomenko categorization is used for identifying all generic LTB in this section. Thus, the definitions below are considered [37].

(i) If there is a simple manifold system M^{2n} with $F : M^{2n} \to R^{2n}$, and $f_1,\ f_2, \ldots, f_n$ as independent integrals, the function $F(x) = (f_1,\ f_2, \ldots, f_n)$ is referred to as momentum mapping.

(ii) If the rank satisfies $dF(x) < n$, and $F(x) \in R^n$, then $x \in M$ is recognized as a critical point of the momentum mapping.

(iii) The bifurcation graph is the set $B = F(k) \subset R^n$ formed by the union of many parts B_k.

(iv) The set of all critical points associated with the momentum mapping Z is contained within the set M.

In the present problem the LS has the topology

$$L_S = \{(q_1, q_2, \dot{q}_1, \dot{q}_2) \in R^4 : H = h, F = \alpha \subset R^4\},$$

where L_S is formed by a finite union of 2-D tori corresponding to non-critical values of F and H. The set of critical points allows for the determination of the energy-momentum diagram.

$$(q_1, q_2, \dot{q}_1, \dot{q}_2) \to (H, F),$$

where D represents the discriminant region of the functions $\phi(q_1)$ and $\phi(q_2)$, where their coefficients are given in terms of h and α

$$D = D_1 \cup D_2 = [(h, \alpha) \in R^2/\text{disc}(\phi(q_1)) = 0] \cup [(h, \alpha) \in R^2/\text{disc}(\phi(q_2)) = 0]. \tag{12}$$

The point (h, α) that passes through D can modify the topological kind of L_S. The set R^2/D comprised of 16 connected parts as depicted in Figure1. As a result, in every connected part of R^2/D, the level set L_S contains the preceding one type. When H and F are noncritical, the level set L_S forms a finite union of lower-dimensional tori [38]. The number of acceptable ovals on the Riemann surface associated to elliptical curves Γ_j determines their numbers, where

$$\Gamma_j : \omega_j = \sqrt{\phi(q_j)}, \quad j = 1, 2.$$

Table1 describes the roots of both $\phi(q_1)$ and $\phi(q_2)$, whereas Table2 illustrates that L_S is either a torus or a set of non-elements [39]].

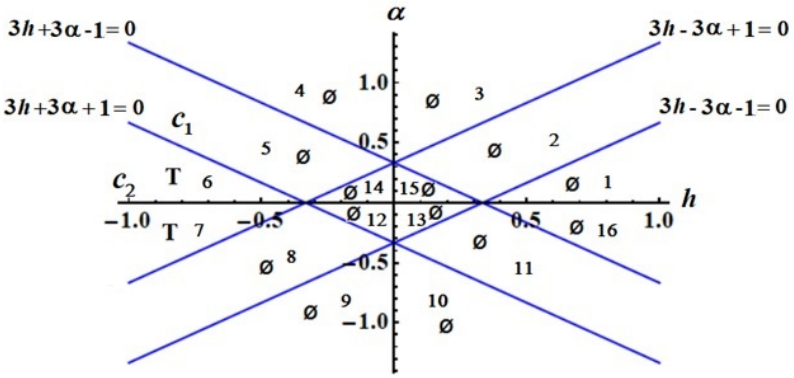

Figure 1: Diagram of bifurcation $D = D_1 \cup D_2$.

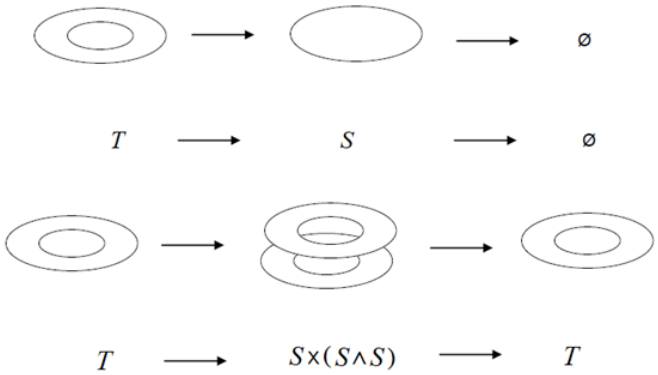

Figure 2: The LTB.

Table 1: Topological class of L_S and the real roots of $\phi(q_1)$ and $\phi(q_2)$ for $(h, \alpha) \in R^2/D$.

Domain	Roots of $\phi(q_1)$	Roots of $\phi(q_2)$
1	0	0
2	0	0
3	$a > 0$	0
4	$a > 0$	0
5	$a > 0$	0
6	$a > 0$	$b > 0$
7	$a > 0$	$b > 0$
8	0	$b > 0$
9	0	$b > 0$
10	0	$b > 0$
11	0	0
12	0	0
13	0	0
14	0	0
15	0	0
16	0	0

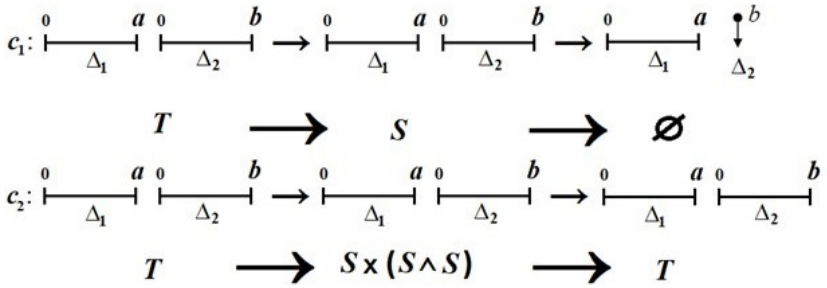

Figure 3: The bifurcations of invariant Liouville tori are linked to the bifurcations of the polynomial roots $\phi(q_1)$ and $\phi(q_2)$.

2.2. Periodic solution

According to the preceding section, we have PS on the specified curve denoted by c_1 where $3(h + \alpha) = -1$. This observation is supported by the data presented in table 4, where the q_1 parameter taking value in interval $[0, a]$ and $q_2 = 2$. Solving equation (11), the function $\phi(z)$ is a third-degree polynomial that has a real root a and two roots d and $\bar{d}$ which are complex

$$\phi(z) = -\frac{z^3}{3} + cz + n = (a - z)(z - d)(z - \bar{d}), \tag{13}$$

and, $n = 2(\alpha - h)$.
Using the following relations

$$(z - d)(z - \bar{d}) = (x - d_1)^2 + a_1^2, \tag{14}$$

Table 2: Allowable ovals on diagram D.

Domain	q_1-planeΔ_1	q_2-planeΔ_2	Topological type
1	$\emptyset$	$\emptyset$	$\emptyset$
2	$[0,a]$	$\emptyset$	$\emptyset$
3	$[0,a]$	$\emptyset$	$\emptyset$
4	$[0,a]$	$\emptyset$	$\emptyset$
5	$[0,a]$	$\emptyset$	$\emptyset$
6	$[0,a]$	$[0,b]$	T
7	$[0,a]$	$[0,b]$	T
8	$\emptyset$	$[0,b]$	$\emptyset$
9	$\emptyset$	$[0,b]$	$\emptyset$
10	$\emptyset$	$[0,b]$	$\emptyset$
11	$\emptyset$	$\emptyset$	$\emptyset$
12	$\emptyset$	$\emptyset$	$\emptyset$
13	$\emptyset$	$\emptyset$	$\emptyset$
14	$\emptyset$	$\emptyset$	$\emptyset$
15	$\emptyset$	$\emptyset$	$\emptyset$
16	$\emptyset$	$\emptyset$	$\emptyset$

Table 3: The generic bifurcations of L_S between domains i and ℓ, where $i=6,7$ and $\ell=(1:5,8:16)$.

$6\to 7$	$6\to \ell$	$7\to \ell$
$T\to T$	$T\to \emptyset$	$T\to \emptyset$

where

$$d_1=\frac{d+\bar{d}}{2},\quad a_1^2=\frac{-(d-\bar{d})^2}{4},\quad (d_1-a)^2+a_1^2=A^2.$$

Then, $\phi(z)$ can be rewritten as

$$\phi(z)=(a-z)\left((z-d_1)^2+a_1^2\right). \tag{15}$$

Taking into account that we can consider that

$$z=a-A\frac{1+\cos\varphi}{1-\cos\varphi};\quad -\infty<z\le a. \tag{16}$$

Referring to equations (15) and (16), then equation (11) becomes

$$\int_0^{\varphi}\frac{d\varphi}{\sqrt{1-k_1^2\sin^2\varphi}}=\sqrt{A}(t-t_0). \tag{17}$$

Table 4: The topological type of L_S on diagram D corresponds to the two no-coplanar circles, denoted as $(S\wedge S)$, which intersect at a single shared point.

Curve	Δ_1	Δ_2	$L_S=\Delta_1\times\Delta_2$
c_1	$[0,a]$	$[0,b]$	S
c_2	$[0,a]$	$[0,b]$	$S\times(S\wedge S)$

Therefore, equation (11) has the following solution

$$z = a - A\frac{1+\mathrm{cn}[\sqrt{A}(t-t_0),k_1]}{1-\mathrm{cn}[\sqrt{A}(t-t_0),k_1]}, \tag{18}$$

where $\cos\varphi = \mathrm{cn}(\sqrt{A}(t-t_0))$, with the period T

$$T = \frac{1}{\sqrt{A}}\mathrm{sn}^{-1}(1,k_1) = \frac{1}{\sqrt{A}}K(k_1), \quad K(k_1) = \int_0^{\pi/2}\frac{d\varphi}{\sqrt{1-k_1^2\sin^2\varphi}},$$

where $K(k_1)$ denotes the complete elliptic integral of the first kind.

2.3. The phase portrait after separation

The phase portrait is a successful tool to get the type of singularity for separated functions. The singularity of the rotation of a RB revolving around a fixed point in the Kovalevskaya case is studied in [40], while in [41] the singular points in the problem of two fixed centers are classified. It is defined that the type of singular point is elliptic, hyperbolic, or parabolic according to the Jacobian. We consider the function

$$F = p^2 + \frac{q^3}{6} - \frac{c}{2}q + h - \alpha. \tag{19}$$

The singular points have been obtained from the following equations,

$$\frac{\partial F}{\partial p} = 2p = 0, \quad \frac{\partial F}{\partial q} = \frac{q^2}{2} - \frac{c}{2} = 0. \tag{20}$$

Then, from equation (20) there exists two singular points $(0, \pm\sqrt{c})$.
In order to determine the type of these points, put $p = x$ and $q = y \pm \sqrt{c}$ in equation (19) and ignoring terms of degree greater than two, thus the point $(0, \sqrt{c})$ is elliptic point where the Jacobian $J = F_{xx}F_{yy} - F_{xy}F_{yx} > 0$, and the point $(0, -\sqrt{c})$ is hyperbolic point where the Jacobian $J = F_{xx}F_{yy} - F_{xy}F_{yx} < 0$ as shown in Figure 4.

3. Separation of the last case of quartic potential

The Hamiltonian function associated with the quartic potential in the last case is given by

$$H = \frac{1}{2}\left(p_x^2 + p_y^2\right) + \alpha(x^4 + 6x^2y^2 + 8y^4), \tag{21}$$

for simplicity, we can consider that $\alpha = 1$. In [28], the authors used the transformation

$$u = \frac{p_x^2 + c}{x^2} + 2x^2 + 4y^2, \quad v = \frac{p_x^2 - c}{x^2} + 2x^2 + 4y^2, \tag{22}$$

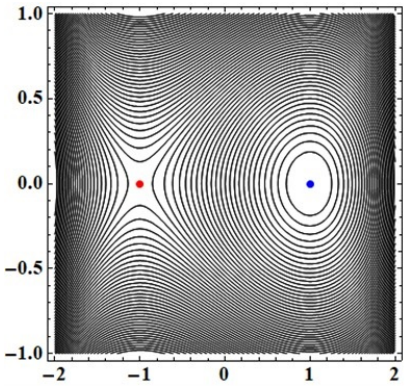

Figure 4: The elliptic point $(0, \sqrt{c})$ and the hyperbolic point $(0, -\sqrt{c})$.

where

$$x^2 = \frac{2c}{u-v}, \quad y^2 = \frac{u+v}{8} - \frac{c}{u-v} - \frac{(\dot{v}-\dot{u})^2}{16(u-v)^2}.$$

Hence the separation equations are written in the form

$$\dot{u}^2 = 2u^3 - 8u(2h+C), \quad \dot{v}^2 = 2v^3 - 8v(2h-C), \tag{23}$$

where h and C represent the energy integral and second invariant integral respectively

$$\int \frac{du}{\sqrt{P_1(u)}} = \int dt, \quad \int \frac{dv}{\sqrt{P_2(v)}} = \int dt, \tag{24}$$

where

$$P_1(u) = 2u^3 - 8u(2h+C), \quad P_2(v) = 2v^3 - 8v(2h-C). \tag{25}$$

3.1. Bifurcation of the problem

Following the method described in subsection 2.1, the LS of this problem possesses the topology

$$A_S = \{(u, v, \dot{u}, \dot{v}) \in R^4 : \ H = h, \ F = C \subset R^4\}. \tag{26}$$

For non-critical values of both F and H, A_S consists of a limited union of 2-D tori.

The calculation of the energy momentum diagram involves the utilization of the set of critical points $(u, v, \dot{u}, \dot{v}) \to (H, F)$.

If G is the discriminant locus of the polynomials $P_1(u)$ and $P_2(v)$, with coefficients depending on h and C, then

$$G = G_1 \cup G_2 = [(h, C) \in R^2/\text{disc}(P_1(u)) = 0] \cup [(h, C) \in R^2/\text{disc}(P_2(v)) = 0]. \tag{27}$$

The set R^2/G is comprised of of eight connected components, as shown in Figure 5. Table 5 indicates the real roots of $P_1(u)$ and $P_2(v)$ aiming to obtain the ovals (a related component for the set of fixed points on the curve Γ_j, $(j = 1, 2)$); where $\Gamma_1 : \omega_1 = \sqrt{P_1(u)}$ and $\Gamma_2 : \omega_2 = \sqrt{P_2(v)}$, while Table 6 shows the topological kind of A_S is a torus, or it

Table 5: Topological type of A_S and real roots of the polynomials $P_1(u)$ and $P_2(v)$ for $(h, C) \in R^2/G$.

Domain	Roots of $P_1(u)$	Roots of $P_2(v)$
1	$u_1 < 0 < u_3$	$v_1 < 0 < v_3$
2	$u_1 < 0 < u_3$	$v_2 = 0$
3	$u_1 < 0 < u_3$	$v_2 = 0$
4	$u_2 = 0$	$v_2 = 0$
5	$u_2 = 0$	$v_2 = 0$
6	$u_2 = 0$	$v_1 < 0 < v_3$
7	$u_2 = 0$	$v_1 < 0 < v_3$
8	$u_1 < 0 < u_3$	$v_1 < 0 < v_3$

might be an empty set. The topological kind is a tours as in D_m $(m = 1, 8)$ or empty as in D_{m^*} $(m^* = 2, 3, 4, 5, 6, 7)$. To analyze all generic LTB of the issue as demonstrated in Table 7, it is sufficient to examine the bifurcations of $P_1(u)$ and $P_2(v)$, the correspondence between invariant LTB and bifurcations of roots of them, see figures 6 and 7.

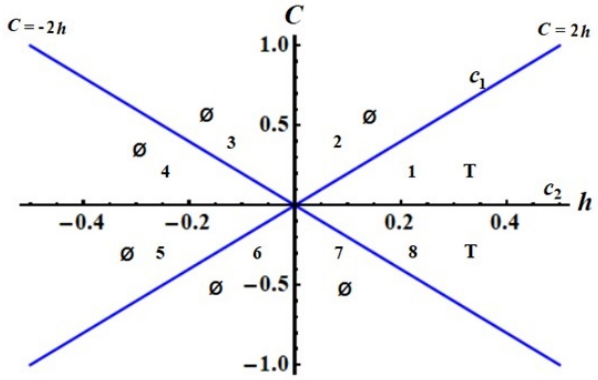

Figure 5: Diagram of bifurcation $G = G_1 \cup G_2$.

3.2. Periodic solution

From the previous section, the PS lies on the curves c_1 where $C = 2h$ as shown in Table 8, and the u_3 parameter taking value in interval $[0, u_3]$ and $v_1 = 0$. According to the initial equation of (25), the function $P_1(u)$ can be characterized as a cubic polynomial whose real roots $u_1, 0$ and u_3. Here

$$P_1(u) = u(u - u_1)(u - u_3); \quad u_3 \leq u, \tag{28}$$

$$u = \frac{u_3}{1 - \sin^2 \varphi}, \tag{29}$$

Table 6: The allowable ovals and the topological classification of A_S for $(h, C) \in R^2/G$.

Domain	$u-$ plane Δ_1	$v-$ plane Δ_2	Topological type
1	$[0, u_3]$	$[v_1, 0]$	T
2	$[0, u_3]$	$\emptyset$	$\emptyset$
3	$[0, u_3]$	$\emptyset$	$\emptyset$
4	$\emptyset$	$\emptyset$	$\emptyset$
5	$\emptyset$	$\emptyset$	$\emptyset$
6	$\emptyset$	$[v_1, 0]$	$\emptyset$
7	$\emptyset$	$[v_1, 0]$	$\emptyset$
8	$[0, u_3]$	$[v_1, 0]$	T

Table 7: The generic bifurcations of A_S between domains i and j, where $i = 1, 8$ and $j = (2 : 7)$.

$T \to T$	$T \to \emptyset$	$T \to \emptyset$

and

$$du = \frac{2u_3 \sin\varphi \cos\varphi}{(1 - \sin^2\varphi)^2} d\varphi. \tag{30}$$

Substituting equations (28)-(30) into the initial equation of (25) to obtain the solution

$$u(t) = \frac{u_3}{1 - \mathrm{sn}^2\left[\frac{n}{2}(t - t_0), k\right]}, \tag{31}$$

with period T

$$T = \frac{2}{n}\mathrm{sn}^{-1}(1, k) = \frac{2}{n}K(k),$$

where

$$K(k) = \int_0^{\pi/2} \frac{d\varphi}{\sqrt{1 - k^2 \sin^2\varphi}}, \quad n = \sqrt{u_3 - u_1}, \quad k^2 = \frac{u_1}{u_1 - u_3}.$$

Here, $K(k)$ represents a complete elliptic integral of the first kind.

3.3. The phase portrait of the separated function

Let the function

$$F = p^2 - 2q^3 + 8q(2h + C). \tag{32}$$

The singular points of F can be determined by evaluating the solutions of the subsequent equations

$$\frac{\partial F}{\partial p} = 2p = 0, \quad \frac{\partial F}{\partial q} = -6q^2 + 8(2h + C) = 0. \tag{33}$$

Table 8: Topological kind of A_S on G.

Curve	Δ_1	Δ_2	$L_S = \Delta_1 \times \Delta_2$
c_1	$[0, u_3]$	$[v_1 = 0]$	S
c_2	$[0, u_3]$	$[v_1, 0]$	$S \times (S \wedge S)$

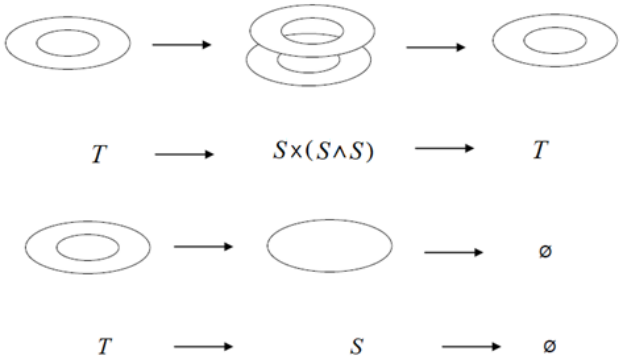

Figure 6: The LTB.

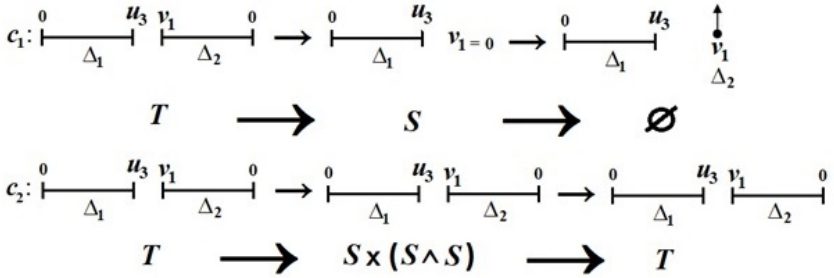

Figure 7: The relation between invariant LTB and bifurcations of roots of $P_1(u)$ and $P_2(v)$.

From equation (33) we have

$$p = 0, \text{ or } q = \pm\sqrt{\frac{8(2h+C)}{6}}.$$

Then, the two singular points $\left(0, \sqrt{\frac{8(2h+C)}{6}}\right)$, $\left(0, -\sqrt{\frac{8(2h+C)}{6}}\right)$.
To identify the types of points, we employ the methodology outlined in subsection 2.3, yielding the subsequent findings

(i) The point $\left(0, \sqrt{\frac{8(2h+C)}{6}}\right)$ is hyperbolic, where $J = G_{xx}G_{yy} - G_{xy}G_{yx} < 0$,

(ii) The point $\left(0, -\sqrt{\frac{8(2h+C)}{6}}\right)$ is elliptic, where $J = G_{xx}G_{yy} - G_{xy}G_{yx} > 0$, as plotted in Figure 8.

4. Periodic solutions by applying Lyapunov's method

The PS close to the equilibrium positions of the systems (1) and (21) are introduced by using Lyapunov's method [42]. Many scientific articles study this method. The problem

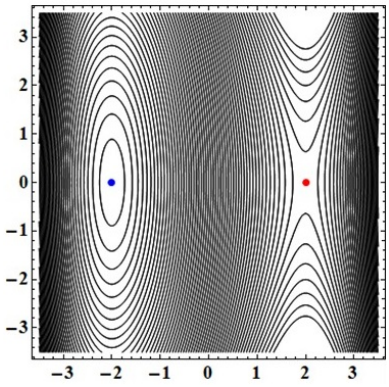

Figure 8: The elliptic point $\left(0, -\sqrt{\frac{8(2h+C)}{6}}\right)$ and the hyperbolic point $\left(0, \sqrt{\frac{8(2h+C)}{6}}\right)$.

of rotating RB around a fixed point is studied in [43–56]. In [44], a new approach to solve the RB problem with constant body torques. In [45], the authors decoupled the Euler equations and solved them with gyrostatic impact. In [46], the problem is solved with time-varying constant body torques. In [51, 52], the author obtained the PS with the energy dissipation that influences the motion.

For the case of generalized HH:

The governing equations for the Hamiltonian (1) governing by the PF V are given by

$$\ddot{X} + V_x = 0, \quad \ddot{Y} + V_y = 0, \tag{34}$$

with the integral related with energy

$$\frac{1}{2}\left(\dot{X}^2 + \dot{Y}^2\right) + V = h. \tag{35}$$

The equilibrium points (X_p, Y_p) can be obtained by solving the equations $V_x = V_y = 0$, such that for each point the equation (35) gives the initial value of the energy constant h. Inserting $X = X_p + \xi,\ Y = Y_p\eta$ in equation (34) to investigate the disturbance motion around the equilibrium points. After some adjustments, the following differential equations may be obtained

$$\ddot{\xi} + L\xi + M\eta = 0, \quad \ddot{\eta} + N\eta + M\xi = 0, \tag{36}$$

where $V_{XX}(X_p, Y_p) = L, \quad V_{YY}(X_p, Y_p) = N, \quad V_{XY}(X_p, Y_p) = M$. Introducing the time transformation

$$u = \nu t, \tag{37}$$

then, the equations (36) become

$$\nu^2 \frac{d^2\xi}{du^2} + L\xi + M\eta = 0, \quad \nu^2 \frac{d^2\eta}{du^2} + N\eta + M\xi = 0. \tag{38}$$

We consider the solution of the system (38) as

$$\xi = \sum_{j=1}^{\infty} \varepsilon^j X^{(j)}, \quad \eta = \sum_{j=1}^{\infty} \varepsilon^j Y^{(j)}, \quad h = h_0 + \sum_{j=2}^{\infty} \varepsilon^j h^{(j)}, \tag{39}$$

where $h^{(j)}$ represent constants and $X^{(j)},\ Y^{(j)}$ express about T-periodic functions of t with the frequency ν that may be formulated as

$$T = \frac{2\pi}{\nu} = \frac{2\pi}{\nu_0}\left(1 + \sum_{j=2}^{\infty} \varepsilon^j T_j\right). \tag{40}$$

Substituting (39) and (40) in (38) and taking the first approximation, then we get

$$\nu_0^2 \frac{d^2X^{(1)}}{du^2} + LX^{(1)} + MY^{(1)} = 0, \quad \nu_0^2 \frac{d^2Y^{(1)}}{du^2} + NY^{(1)} + MX^{(1)} = 0. \tag{41}$$

In order to accomplish our objective, we express the supposed solution for equations (41) in the Fourier series

$$\begin{aligned} X^{(s)} &= a_{1s}^0 + \sum_{r=1}^{s} (a_{1s}^{(r)} \cos ru + b_{1s}^{(r)} \sin ru), \\ Y^{(s)} &= a_{2s}^0 + \sum_{r=1}^{s} (a_{2s}^{(r)} \cos ru + b_{2s}^{(r)} \sin ru), \end{aligned} \tag{42}$$

by taking first approximation of expressions (42) and substituting into (41), then we get the following solutions

$$\begin{aligned} &X = X_p + \varepsilon[\tilde{b}(\nu_0^2 - N)\cos u + \tilde{a}M \sin u], \\ &Y = Y_p + \varepsilon[\tilde{b}M \cos u + \tilde{a}(\nu_0^2 - L)\sin u], \\ &h = h_0 + \tfrac{\varepsilon^2}{4}\Big((\tilde{a}^2 + \tilde{b}^2)\nu_0^6 + (\tilde{a}^2(N - 2L) + \tilde{b}^2(\alpha - 2\beta))\nu_0^4 + \\ &(\tilde{a}^2(L^2 - 2LN + 3M^2) + \tilde{b}^2(N^2 - 2LN + 3M^2))\nu_0^2 + (\tilde{a}^2 L + \tilde{b}^2 N)(LN - M^2)\Big), \end{aligned} \tag{43}$$

where $\tilde{a}$ and $\tilde{b}$ are unrestricted variables. The system's frequency is determined by

$$\nu_0 = \sqrt{\frac{(L+N) \pm \sqrt{(L+N)^2 - 4(LN - M^2)}}{2}}. \tag{44}$$

Taking into account that, the frequency's value ν_0 relies on the values of $L,\ M$ and N. So, let's discuss this scenario.

(i) If $LN - M^2 < 0$, this means that the equilibrium points (X_p, Y_p) are saddle points. In the current case, one family of periodic orbits close to the equilibrium points with the frequency (44) in a positive sign is obtained.

(ii) If $LN - M^2 > 0$, which means that there is an extremum value for the PF at (X_p, Y_p). The inequality $L + N > 2\sqrt{LN - M^2}$ with the second condition produce the criteria for the stability of the equilibrium (X_p, Y_p), where the roots of the frequency are pure imaginary, consequently we get two families of PS around the minimum stable points.

For the case of quartic potential:
The PS can be obtained by the same steps as the previous steps. The governing equations for the Hamiltonian (21) may be represented as follows

$$\ddot{x} + V_x = 0, \quad \ddot{y} + V_y = 0, \tag{45}$$

and these equations satisfy the energy integral

$$\frac{1}{2}\left(\dot{x}^2 + \dot{y}^2\right) + V = h. \tag{46}$$

Moreover, the equilibrium points (x_p, y_p) can be obtained by solving the equations $V_x = V_y = 0$, in which from equation (46) there is an initial value of the energy constant h for each equilibrium point.

Inserting $x = x_p + \xi,\ y = y_p + \eta$ into equation (45), we get after some calculations the following linear equations

$$\ddot{\xi} + \gamma\xi + \mu\eta = 0, \quad \ddot{\eta} + \kappa\eta + \mu\xi = 0, \tag{47}$$

where $V_{xx}(x_p, y_p) = \gamma, \quad V_{yy}(x_p, y_p) = \kappa, \quad V_{xy}(x_p, y_p) = \mu$.

Introducing the time transformation, $(u = \nu t)$ and following the same steps in equations (38)-(40) and taking the first approximation, then we get

$$\nu_0^2 \frac{d^2x^{(1)}}{du^2} + \gamma x^{(1)} + \mu y^{(1)} = 0, \quad \nu_0^2 \frac{d^2y^{(1)}}{du^2} + \kappa y^{(1)} + \mu x^{(1)} = 0. \tag{48}$$

As well known the solution of (48) can be obtained using the Fourier series

$$\begin{aligned} x^{(s)} &= a_{1s}^0 + \sum_{r=1}^{s} (a_{1s}^{(r)} \cos ru + b_{1s}^{(r)} \sin ru), \\ y^{(s)} &= a_{2s}^0 + \sum_{r=1}^{s} (a_{2s}^{(r)} \cos ru + b_{2s}^{(r)} \sin ru). \end{aligned} \tag{49}$$

Setting the first approximation of expressions (49) into (48), then we get the following solutions

$$\begin{aligned} &x = x_p + \varepsilon[\tilde{B}(\nu_0^2 - \kappa)\cos u + \tilde{A}\mu \sin u], \\ &y = y_p + \varepsilon[\tilde{B}\mu \cos u + \tilde{A}(\nu_0^2 - \gamma)\sin u], \\ &h = h_0 + \tfrac{\varepsilon^2}{4}\Big((\tilde{A}^2 + \tilde{B}^2)\nu_0^6 + (\tilde{A}^2(\kappa - 2\gamma) + \tilde{B}^2(\gamma - 2\kappa))\nu_0^4 + \\ &(\tilde{A}^2(\gamma^2 - 2\gamma\kappa + 3\mu^2) + \tilde{B}^2(\kappa^2 - 2\gamma\kappa + 3\mu^2))\nu_0^2 + (\tilde{A}^2\gamma + \tilde{B}^2\kappa)(\gamma\kappa - \mu^2)\Big), \end{aligned} \tag{50}$$

where $\tilde{A}$ and $\tilde{B}$ are undefined chosen parameters. The frequency is given by

$$\nu_0 = \sqrt{\frac{(\gamma + \kappa) \pm \sqrt{(\gamma + \kappa)^2 - 4(\gamma\kappa - \mu^2)}}{2}}. \tag{51}$$

Thus, there are two types of equilibrium points:

(i) If $\gamma\kappa - \mu^2 < 0$, this means that the points (x_p, y_p) of equilibrium are saddle points, which give a family of PS with the positive sign of frequency (51).

(ii) If $\gamma\kappa - \mu^2 > 0$, the equilibrium points (x_p, y_p) are either minimum or maximum for the PF (2). This condition with the inequality $\gamma + \kappa > 2\sqrt{\gamma\kappa - \mu^2}$ gives the equilibrium stability condition (x_p, y_p) (i.e., the roots of the frequency are pure imaginary), consequently there are two families of PS around the minimum stable points.

5. Conclusion

The present study investigates the comprehensive characterization of two galactic motion models. The topological type of the LS is introduced, which is a torus or an empty set. Moreover, the PS of the two models is obtained. The phase portrait of separated functions is analyzed and through it, we get the singular points that are elliptic and hyperbolic. The elliptic points are found to exhibit stability, while the remaining points demonstrate instability. The Lyapunov theorem [42] is applied to study the PS. Moreover, we have obtained two families of PS around the stable equilibrium point, whereas each PF has one family that is near to the saddle points. The outcomes of this research are applicable in celestial mechanics and astrodynamics, particularly for modeling gravitational interactions between celestial bodies like planets and asteroids. By classifying singular points and examining phase portraits, the study also provides tools for understanding chaotic behaviors in weather forecasting and economic modeling. Additionally, the analysis of bifurcations and PS supports advancements in robotics and automation systems.

Authors Statements

T. S. Amer: Methodology, Data curation, Visualization, Conceptualization, Writing, Reviewing, Editing.
F. M. El-Saba: Methodology, Validation, Visualization, Conceptualization.
M. Fakharany: Methodology, Conceptualization, Resources, Reviewing.
H. M. Gad: Methodology, Conceptualization, Investigation, Data curation, Writing - original draft.

Conflict of Interest

The authors declare that they have no conflict of interest.

Funding Acknowledgement

This research received no specific grant from any funding agency in the public, commercial, or not-for-profit sectors.

Data Availability

Data sharing not applicable to this article as no datasets were generated or analyzed during the current study.

References

[1] Michel Hénon and Carl Heiles. The applicability of the third integral of motion: some numerical experiments. *Astronomical Journal*, 69:73–79, 1964.

[2] G. Contopoulos and C. Polymilis. Approximations of the 3-particle toda lattice. *Physica D: Nonlinear Phenomena*, 24(1-3):328–342, 1987. Publisher: Elsevier BV.

[3] Morikazu Toda. Vibration of a Chain with Nonlinear Interaction. *Journal of the Physical Society of Japan*, 22(2):431–436, 1967. Publisher: Physical Society of Japan.

[4] Dante Carrasco and Claudio Vidal. Periodic Solutions, Stability and Non-Integrability in a Generalized Hénon-Heiles Hamiltonian System. *Journal of Nonlinear Mathematical Physics*, 20(2):199, 2021. Publisher: Springer Science and Business Media LLC.

[5] Philip Holmes. Proof of non-integrability for the Hénon-Heiles Hamiltonian near an exceptional integrable case. *Physica D: Nonlinear Phenomena*, 5(2-3):335–347, September 1982. Publisher: Elsevier BV.

[6] Jaume Llibre and Lidia Jiménez-Lara. Periodic orbits and non-integrability of Hénon–Heiles systems. *Journal of Physics A: Mathematical and Theoretical*, 44(20):205103, 2011. Publisher: IOP Publishing.

[7] Mordechai Bixon and Joshua Jortner. Quantum dynamics of the Henon–Heiles system. *The Journal of Chemical Physics*, 77(8):4175–4187, 1982. Publisher: AIP Publishing.

[8] A.I. Akhiezer, V.I. Truten', and N.F. Shul'ga. Dynamic chaos in the motion of charged particles through a crystal. *Physics Reports*, 203(5), May 1991. Publisher: Elsevier BV.

[9] R. Rajaraman and Erick J. Weinberg. Internal symmetry and the semiclassical method in quantum field theory. *Physical Review D*, 11(10):2950–2966, 1975. Publisher: American Physical Society (APS).

[10] R. Dutt and M. Lakshmanan. Application of coherent state representation to classical $x6$ and coupled anharmonic oscillators. *Journal of Mathematical Physics*, 17(4):482–484, 1976. Publisher: AIP Publishing.

[11] R. Friedberg, T. D. Lee, and A. Sirlin. Class of scalar-field soliton solutions in three space dimensions. *Physical Review D*, 13(10):2739–2761, 1976. Publisher: American Physical Society (APS).

[12] Giuseppe Pucacco, Dino Boccaletti, and Cinzia Belmonte. Quantitative predictions with detuned normal forms. *Celestial Mechanics and Dynamical Astronomy*, 102(1-3):163–176, 2008. Publisher: Springer Science and Business Media LLC.

[13] Dieter Armbruster, John Guckenheimer, and Seunghwan Kim. Chaotic dynamics in systems with square symmetry. *Physics Letters A*, 140(7-8):416–420, 1989. Publisher: Elsevier BV.

[14] E Calzetta and C El Hasi. Chaotic Friedmann-Robertson-Walker cosmology. *Classical and Quantum Gravity*, 10(9):1825–1841, 1993. Publisher: IOP Publishing.

[15] B. Grammaticos, B. Dorizzi, and R. Padjen. Painleve property and integrals of motion for the Henon-Heiles system. *Physics Letters A*, 89(3):111–113, 1982. Publisher: Elsevier BV.

[16] M. Lakshmanan and R. Sahadevan. Painlevé analysis, Lie symmetries, and integrability of coupled nonlinear oscillators of polynomial type. *Physics Reports*, 224(1-2):1–93, 1993. Publisher: Elsevier BV.

[17] Tassos Bountis, Harvey Segur, and Franco Vivaldi. Integrable Hamiltonian systems and the Painlevé property. *Physical Review A*, 25(3):1257–1264, 1982. Publisher: American Physical Society (APS).

[18] S. Kasperczuk. Integrability of the Yang-Mills Hamiltonian system. *Celestial Mechanics & Dynamical Astronomy*, 58(4):387–391, 1994. Publisher: Springer Science and Business Media LLC.

[19] A. Ramani, B. Dorizzi, and B. Grammaticos. Painlevé Conjecture Revisited. *Physical Review Letters*, 49(21):1539–1541, 1982. Publisher: American Physical Society (APS).

[20] Stefan Wojciechowski. Separability of an integrable case of the Henon-Heiles system. *Physics Letters A*, 100(6):277–278, 1984. Publisher: Elsevier BV.

[21] Edmund T. Whittaker. *A treatise on the analytical dynamics of particles and rigid bodies: with an introduction to the problem of three bodies.* Cambridge Mathematical Library. Cambridge Univ. Press, Cambridge, 4. ed., transferred to digital print edition, 1999.

[22] B. Dorizzi, B. Grammaticos, and A. Ramani. A new class of integrable systems. *Journal of Mathematical Physics*, 24(9):2282–2288, 1983. Publisher: AIP Publishing.

[23] Katsuya Nakagawa and Haruo Yoshida. A list of all integrable two-dimensional homogeneous polynomial potentials with a polynomial integral of order at most four in the momenta. *Journal of Physics A: Mathematical and General*, 34(41):8611–8630, 2001. Publisher: IOP Publishing.

[24] C. Verhoeven, M. Musette, and R. Conte. Integration of a generalized Hénon–Heiles Hamiltonian. *Journal of Mathematical Physics*, 43(4):1906–1915, 2002. Publisher: AIP Publishing.

[25] V. Ravoson, A. Ramani, and B. Grammaticos. Generalized separability for a Hamiltonian with nonseparable quartic potential. *Physics Letters A*, 191(1-2):91–95, 1994. Publisher: Elsevier BV.

[26] Pol Vanhaecke. *Explicit techniques for studying two-dimensional integrable systems.* PhD thesis, 1991.

[27] A. T. Fomenko. *Integrability and Nonintegrability in Geometry and Mechanics.*

Springer Netherlands, Dordrecht, 1988.

[28] F. M. El-Sabaa, M. Hosny, and S. K. Zakria. Bifurcations of Liouville tori of a two fixed center problem. *Astrophysics and Space Science*, 363(4), 2018. Publisher: Springer Science and Business Media LLC.

[29] F. M. El-Sabaa, M. Hosny, and S. K. Zakria. Bifurcations of Armbruster Guckenheimer Kim galactic potential. *Astrophysics and Space Science*, 364(2):1–9, 2019. Publisher: Springer Science and Business Media LLC.

[30] Holger Waalkens, Holger R. Dullin, and Peter H. Richter. The problem of two fixed centers: bifurcations, actions, monodromy. *Physica D: Nonlinear Phenomena*, 196(3-4):265–310, 2004. Publisher: Elsevier BV.

[31] Mikhail P Kharlamov. Bifurcation of common levels of first integrals of the kovalevskaya problem. *Journal of Applied Mathematics and Mechanics*, 47(6):737–743, 1983.

[32] A Ouazzani-Th, J Kharbach, and M Ouazzani-Jamil. Phase space topology and bifurcation of liouville torii in the goryatchev-tchaplygin top. *Moroccan Journal of Condensed Matter*, 2, 1999.

[33] TS Amer. On the rotational motion of a gyrostat about a fixed point with mass distribution. *Nonlinear Dynamics*, 54(3):189–198, 2008.

[34] TS Amer. The rotational motion of the electromagnetic symmetric rigid body. *Appl. Math. Inf. Sci*, 10(4):1453–1464, 2016.

[35] AA Galal, TS Amer, AH Elneklawy, and HF El-Kafly. Studying the influence of a gyrostatic moment on the motion of a charged rigid body containing a viscous incompressible liquid. *The European Physical Journal Plus*, 138(10):1–13, 2023.

[36] Allan P Fordy. The hénon-heiles system revisited. *Physica D: Nonlinear Phenomena*, 52(2-3):204–210, 1991.

[37] Boris A. Dubrovin, Anatolij Timofeevič Fomenko, and Sergeĭ Petrovich Novikov. *Modern Geometry—Methods and Applications: Part II: The Geometry and Topology of Manifolds*. Springer Science & Business Media, 1985.

[38] Vladimir Igorevich Arnol'd. *Mathematical methods of classical mechanics*, volume 60. Springer Science & Business Media, 2013.

[39] Anatolij T Fomenko. *Visual geometry and topology*. Springer Science & Business Media, 2012.

[40] FM El-Sabaa. Bifurcation of kovalevskaya polynomial. *International Journal of Theoretical Physics*, 34(10), 1995.

[41] FM El-Sabaa, M Hosny, and SK Zakria. Bifurcations of liouville tori of generalized two-fixed center problem. *Italian Journal of Pure and Applied Mathematics*, 43:331–352, 2020.

[42] Aleksandr Mikhailovich Lyapunov. The general problem of the stability of motion. *International journal of control*, 55(3):531–534, 1992.

[43] TS Amer, HF El-Kafly, AH Elneklawy, and AA Galal. Analyzing the dynamics of a charged rotating rigid body under constant torques. *Scientific Reports*, 14(1):9839, 2024.

[44] Amer TS, Elneklawy AH, and El-Kafly HF. A novel approach to solving euler's

nonlinear equations for a 3dof dynamical motion of a rigid body under gyrostatic and constant torques. *Journal of Low Frequency Noise, Vibration and Active Control*, 44(1):111–129, 2025.

[45] TS Amer and IM Abady. Solutions of euler's dynamic equations for the motion of a rigid body. *Journal of Aerospace Engineering*, 30(4):04017021, 2017.

[46] TS Amer, AH Elneklawy, and HF El-Kafly. Analysis of euler's equations for a symmetric rigid body subject to time-dependent gyrostatic torque. *Journal of Low Frequency Noise, Vibration and Active Control*, page 14613484241312465, 2025.

[47] TS Amer, AM Farag, and WS Amer. The dynamical motion of a rigid body for the case of ellipsoid inertia close to ellipsoid of rotation. *Mechanics Research Communications*, 108:103583, 2020.

[48] TS Amer, H Elkafly, and AA Galal. The 3d motion of a charged solid body using the asymptotic technique of kbm. *Alexandria Engineering Journal*, 60(6):5655–5673, 2021.

[49] TS Amer, HF El-Kafly, AH Elneklawy, and WS Amer. Modeling analysis on the influence of the gyrostatic moment on the motion of a charged rigid body subjected to constant axial torque. *Journal of Low Frequency Noise, Vibration and Active Control*, 43(4):1593–1610, 2024.

[50] Asmaa Amer, TS Amer, and AA Galal. Simulation of a subjected rigid body motion to an external force and moment. *Journal of Vibration Engineering & Technologies*, 12(3):2775–2790, 2024.

[51] TS Amer, HF El-Kafly, AH Elneklawy, and AA Galal. Stability analysis of a rotating rigid body: The role of external and gyroscopic torques with energy dissipation. *Journal of Low Frequency Noise, Vibration and Active Control*, page 14613484251324586, 2025.

[52] TS Amer, AH Elneklawy, and HF El-Kafly. Dynamical motion of a spacecraft containing a slug and influenced by a gyrostatic moment and constant torques. *Journal of Low Frequency Noise, Vibration and Active Control*, page 14613484251322235, 2025.

[53] FM El-Sabaa, TS Amer, HM Gad, and MA Bek. Existence of periodic solutions and their stability for a sextic galactic potential function. *Astrophysics and Space Science*, 366(8):74, 2021.

[54] TS Amer, Asma Alanazy, AH Elneklawy, WS Amer, and HF El-Kafly. A novel study on the fourth first integral for the rotatory motion of an impacted charged rigid body by external torques. *Journal of Low Frequency Noise, Vibration and Active Control*, page 14613484251347080, 2025.

[55] TS Amer, HF El-Kafly, AH Elneklawy, and AA Galal. Analyzing the spatial motion of a rigid body subjected to constant body-fixed torques and gyrostatic moment. *Scientific Reports*, 14(1):5390, 2024.

[56] TS Amer, WS Amer, M Fakharany, AH Elneklawy, and HF El-Kafly. Modeling of the euler-poisson equations for rigid bodies in the context of the gyrostatic influences: an innovative methodology. *European Journal of Pure and Applied Mathematics*, 18(1):5712–5712, 2025.